ELSEVIER

Inorganica Chimica Acta 270 (1998) 77–86

Inorganica Chimica Acta

Thermal and photochemical substitution reactions of $CpRe(PPh_3)_2H_2$ and $CpRe(PPh_3)H_4$. Catalytic insertion of ethylene into the C–H bond of benzene

William D. Jones *, John A. Maguire, Glen P. Rosini

Department of Chemistry, University of Rochester, Rochester, NY 14627, USA

Received 28 February 1997; accepted 21 April 1997

Abstract

The thermal and photochemical reactions of $CpRe(PPh_3)_2H_2$ and $CpRe(PPh_3)H_4$ ($Cp=\eta^5$-C_5H_5) with PMe_3, P(*p*-tolyl)$_3$, PMe_2Ph, DMPE, DPPE, DPPM, CO, 2,6-xylylisocyanide and ethylene have been examined. While $CpRe(PPh_3)_2H_2$ is thermally inert, it will undergo photochemical substitution of one or two PPh_3 ligands. With ethylene, substitution is followed by insertion of the olefin into the C–H bond of benzene, giving ethylbenzene. $CpRe(PPh_3)H_4$ undergoes thermal loss of PPh_3, which leads to substituted products of the type $CpRe(L)H_4$. Photochemically, reductive elimination of dihydrogen occurs preferentially. The complex *trans*-$CpRe(DMPE)H_2$ was structurally characterized, crystallizing in the monoclinic space group $P2_1/n$ (No. 14) with $a=6.249(6)$, $b=16.671(8)$, $c=13.867(7)$ Å, $\beta=92.11(6)°$, $V=1443.7(2.9)$ Å^3 and $Z=4$. The complex *trans*-$CpRe(PMe_2Ph)_2H_2$ was structurally characterized, crystallizing in the monoclinic space group $P2_1/n$ (No. 14) with $a=7.467(3)$, $b=23.874(14)$, $c=11.798(6)$ Å, $\beta=100.16(4)°$, $V=2070.2(3.4)$ Å^3 and $Z=4$. © 1998 Elsevier Science S.A.

Keywords: Crystal structures; Catalytic insertion; Rhenium complexes; Cyclopentadienyl complexes; Hydride complexes

1. Introduction

Ephritikhine and co-workers first produced $CpRe(PPh_3)_2H_2$ (**1**), as the C–H activation product resulting from the thermal reaction of $Re(PPh_3)_2H_7$ and cyclopentane, cyclopentene or cyclopentadiene [1]. $CpRe(PPh_3)_2H_2$ acts as the thermodynamic sink in these reactions, and consistent with these results complex **1** has been found to be of limited utility in the preparation of new complexes. Ephritikhine and co-workers also observed that **1** is protonated by strong acids, HX, to yield $[CpRe(PPh_3)_2H_3]X$ [2]. Thermally, **1** is quite stable and only slowly decomposes in air over several weeks.

Although the thermal reactivity of **1** was limited, its photochemistry is more versatile. It has been demonstrated to act as a photocatalyst for H/D exchange between C_6D_6 and alkanes [3]. A related complex, $CpRe(PPh_3)H_4$ (**2**), has also been prepared and found to be thermally and photochemically reactive [4]. Both **1** and **2** can be prepared from the precursor (η^4-C_5H_6)$Re(PPh_3)_2H_3$, which thermally loses H_2 to produce **1** or photochemically loses PPh_3 to produce **2** (Eq. (1)) [5]. This paper extends the thermal and photochemistry of complexes **1** and **2**, and shows how ethylene can be catalytically inserted into the C–H bonds of benzene.

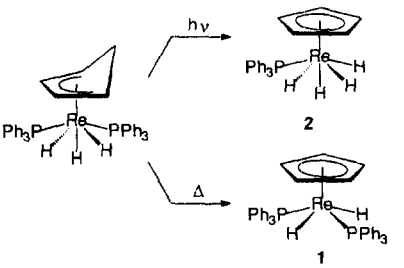

(1)

2. Results and discussion

2.1. Thermal reactivity of 1

A solution of $CpRe(PPh_3)_2H_2$ in C_6D_6 fails to show any evidence of reaction or decomposition when analyzed by ^1H NMR spectroscopy after heating to 220°C in a sealed tube for 24 h. When a C_6D_6 solution of **1** was heated (220°C) in the presence of PMe_3 (20 equiv.), still no reaction was observed after 25 h. The lack of phosphine substitution prod-

* Corresponding author. Tel.: + 1-716-275 5493; fax: + 1-716-473 6889.

PII S0020-1693(97)05828-3

ucts in this reaction eliminates the possibility that PPh_3 is rapidly and reversibly lost from **1** via the 16-electron intermediate, $[CpRe(PPh_3)H_2]$.

The reaction of **1** (4.4 mM) with bromomethane (10 equiv.) at 95°C in C_6D_6 solution produces a single halogenation product, with proton NMR resonances at δ 7.601 (m, 12H), 6.980 (m, 18H), 4.430 (s, 5H) and −10.000 (t, J= 42.3 Hz, 1H) which integrate correctly for $CpRe(Br)(PPh_3)_2H$ and methane (δ 0.148, s), in quantitative yield after 20 days (Eq. (2)).

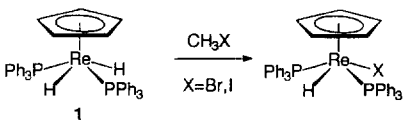

1 (2)

The reaction of **1** with iodomethane under the same conditions also produces methane and a single organometallic product with ^1H NMR resonances whose integrations are consistent with the formation of $CpRe(I)(PPh_3)_2H$. Attempts to generate $CpRe(R)(PPh_3)_2H$ (R = methyl, t-butyl, phenyl) complexes by reaction of the $CpRe(X)(PPh_3)_2H$ complexes with Grignard or lithium reagents produced no reaction. Addition of $AgPF_6$ (1 equiv.) to the solution to facilitate substitution of R for X failed to labilize the halide and instead produced a deep red sparingly soluble product which may be the result of oxidation by Ag^+ to yield a $[CpRe(X)(PPh_3)_2H]^+$ cation. Complex **1** is known to undergo reversible 1 e^- oxidation [6]. The lack of thermal reactivity of **1** led to exploration of its photochemical reactivity.

2.2. Photosubstitution reactions of 1

The UV–Vis spectrum of **1** in THF solution shows a well defined absorption maximum at 328 nm (ϵ = 7200 M^{-1} cm^{-1}), just above the Pyrex glass UV cutoff at about 300 nm. Irradiation of a C_6D_6 solution of **1** (4.4 mM) and $P(p\text{-tolyl})_3$ (22 mM) shows free PPh_3 and mono- and bis-phosphine substitution products, $CpRe(PPh_3)[P(p\text{-tolyl})_3]H_2$, and $CpRe[P(p\text{-tolyl})_2]_2H_2$. The photosubstitution of phosphine is general and includes both alkyl and aryl phosphines, as well as the chelating phosphines DMPE, DPPE and DPPM. Several other two electron donors including CO, isonitrile and ethylene are also substituted for phosphine upon photolysis of **1**. Table 1 gives a compilation of ^1H NMR data for these complexes, and Scheme 1 summarizes these reactions.

All of the $CpReL_2H_2$ complexes presumably exhibit *trans* hydrides, in the case of the phosphine containing complexes, based on the observed P–H coupling constants. For bis-phosphine complexes the triplet coupling is between 40 and 48 Hz, and for the mono-phosphine complexes the P–H coupling of the hydride doublet is 18 to 22 Hz. The *trans* geometry was observed in the previously determined structure of $CpRe(PPh_3)_2H_2$ [4]. The complex $CpRe(PMe_2Ph)_2H_2$ was also examined by X-ray diffraction and found to be a *trans* product (Fig. 1). The hydride ligands were located and

Table 1
^1H NMR data for rhenium complexes in C_6D_6 solvent

Compound	Chemical shift, δ (multiplicity, J, area)
$CpRe(PPh_3)_2H_2$	7.620 (m, 12H), 6.973 (m, 18H), 4.268 (s, 5H), −9.952 (t, J=40.1 Hz, 2H)
$CpRe(Br)(PPh_3)_2H$	7.601 (t, J=7.2 Hz, 12H), 6.98 (m, 18H), 4.430 (s, 5H), −10.000 (t, J=42.3 Hz, 1H)
$CpRe(I)(PPh_3)_2H$	7.545 (t, J=7.2 Hz, 12H), 6.98 (m, 18H), 4.433 (s, 5H), −10.830 (t, J=48.7 Hz, 1H)
$CpRe(PPh_3)(PMe_3)H_2$	7.800 (m, 6H), 7.060 (m, 9H), 4.531 (s, 5H), 1.218 (d, J=8.9 Hz, 9H), −11.186 (dd, J=44.7, 40.7 Hz, 2H)
$CpRe(PMe_3)_2H_2$	4.455 (s, 5H), 1.536 (d, J=7.3 Hz, 18H), −12.125 (t, J=43.2 Hz, 2H)
$CpRe(PPh_3)[P(p\text{-tolyl})_3]H_2$	7.680 (m, 6H), 7.351 (m, 6H), 6.95 (m, 15H), 4.342 (s, 5H), 2.040 (s, 9H), −9.923 (t, J=40.1 Hz, 2H)
$CpRe[P(p\text{-tolyl})_3]_2H_2$	7.641 (t, J=9.0 Hz, 12H), 6.902 (t, J=9.0 Hz, 12H), 4.404 (s, 5H), 2.031 (s, 18H), −9.901 (t, J=40.2 Hz, 2H)
$CpRe(PMe_2Ph)_2H_2$	δ 7.55 (t, J=8.3 Hz, 4H), 7.14 (m, 4H), 7.00 (t, J=6.9 Hz, 2H), 4.38 (s, 5H), 1.72 (d, J=8.3 Hz, 12H), −11.54 (t, J=42.4 Hz, 2H)
$CpRe(PPh_3)(CO)H_2$	7.590 (m, 6H), 6.993 (m, 9H), 4.323 (s, 5H), −9.461 (d, J=48.0, 2H)
$CpRe(CO)_2H_2$	4.368 (s, 5H), −9.670 (s, 2H)
$CpRe(PPh_3)(THF)H_2$ (−70°C, THF-d_8)	4.534 (s, 5H), −10.11 (d, J=11.3 Hz, 2H), (PPh_3 obscured)
$CpRe(\eta^1\text{-DMPE})(PPh_3)H_2$	7.80 (m, 6H), 7.00 (m, 9H), 4.524 (s, 5H), 1.602 (pt, J=2.7 Hz, 6H), 1.064 (pt, J=2.6 Hz, 6H), 1.20 (broad m, 4H), −11.233 (dd, J=43.1, 40.7 Hz, 2H)
trans-$CpRe(DMPE)H_2$	4.662 (s, 5H), 1.594 (t, J=8.7 Hz, 12H), 1.148 (d, J=11.6 Hz, 4H), −13.440 (t, J=45.0, 2H)
cis-$CpRe(DMPE)H_2$	4.694 (s, 5H), 1.732 (t, J=8.7 Hz, 6H), 1.234 (t, J=8.7 Hz, 6H), 1.089 (broad m, 4H), −12.640 (broad t, J=18.9 Hz, 2H)
cis-$CpRe(DPPM)H_2$	8.022 (m, 4H), 7.610 (m, 4H), 7.02 (m, 12H), 6.091 (q, J=11.6 Hz, 1H), 5.000 (q, J=11.6 Hz, 1H), 4.607 (s, 5H), −9.959 (dd, J=20.3, 11.6 Hz, 2H)
$CpRe(PPh_3)(CN\text{-}2,6\text{-xylyl})H_2$	7.680 (m, 6H), 6.96 (m, 12H), 2.283 (s, 6H), −9.290 (d, J=46.5 Hz, 2H)
$CpRe(CN\text{-}2,6\text{-xylyl})_3$	6.828 (m, 9H), 5.093 (s, 5H), 2.388 (s, 18H)
$CpRe(PPh_3)H_4$	7.70 (m, 6H), 7.00 (m, 9H), 4.291 (s, 5H), −7.954 (d, J=19.0 Hz, 4H)
$CpRe(PMe_3)H_4$	4.344 (s, 5H), 1.284 (d, J=8.7 Hz, 9H), −8.552 (d, J=20.3 Hz, 4H)
$CpRe(PMe_2Ph)H_4$	δ 7.38 (t, J=8.3 Hz, 2H), 7.05 (m, 2H), 6.98 (t, J=6.9 Hz, 1H), 4.24 (qn, J=0.7 Hz, 5H), 1.72 (d, J=8.3 Hz, 6H), −8.36 (br d, J=20.2 Hz, 4H)
$CpRe[P(p\text{-tolyl})_3]H_4$	7.611 (m, 6H), 6.98 (m, 6H), 1.889 (s, 9H), −7.873 (d, J=19.0 Hz, 4H)

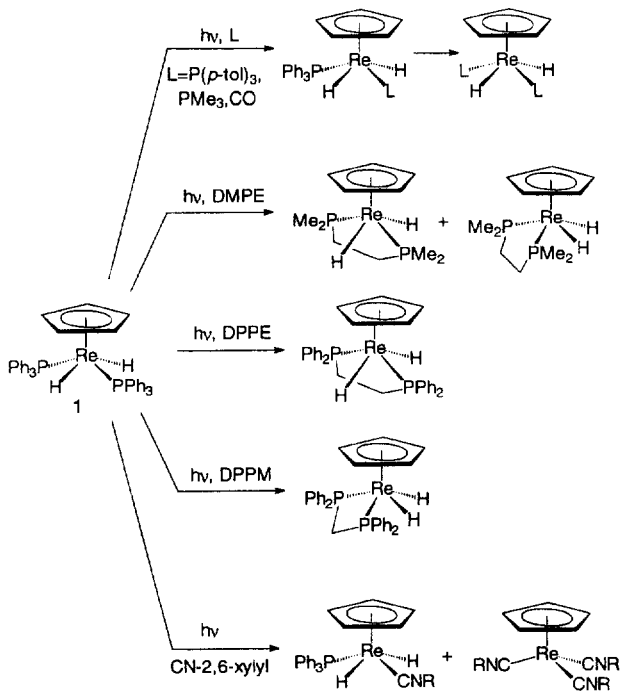

Scheme 1.

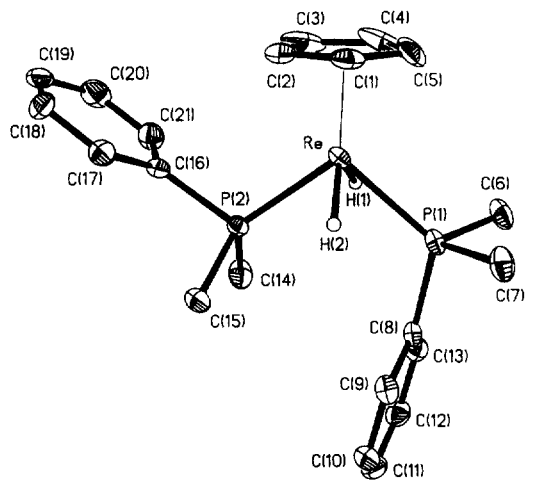

Fig. 1. ORTEP drawing of *trans*-CpRe(PMe_2Ph)$_2H_2$ with ellipsoids shown at the 50% probability level. Hydrogen atoms attached to carbon have been omitted for clarity. The hydride ligands were located and refined.

refined isotropically. The P–Re–P and H–Re–H bond angles of 103.0 and 120°, respectively, compare to values of 108.6 and 138° observed in CpRe(PPh_3)$_2H_2$. The larger P–Re–P angle in **1** can be attributed to the larger cone angle of PPh_3.

The complexes produced from substitution of chelating phosphines are more interesting. The bidentate ligands were expected to force the *cis* disposition of the phosphines and hydrides. A geometry with *cis*-hydrides might be photolabile towards H_2 loss to generate [CpRe(P–P)], a low valent 16-electron intermediate that might be a good candidate as a C–H activation precursor complex for alkanes or arenes. Bergman et al. have used the photogenerated [CpRe(PMe_3)$_2$] intermediate to activate alkanes [7]. The photosubstitution of PPh_3 by DMPE gives a mixture of two isomers (Scheme 1). ^{1}H NMR spectroscopic data for these isomers are compiled in Table 1, and integrate to a 2:1 *trans* to *cis*-phosphine ratio of the complex CpRe(DMPE)H_2 in the crude reaction mixture. Green and co-workers have published other examples of *trans* DMPE complexes, including *trans*-(η^6-toluene)WH_2 [8] and *trans*-(η^6-C_6H_6)Mo(DMPE)H_2 [9]. *Trans*-Ru(C_5Me_5)(DIPPE)H_2^+ is also known [10].

A single crystal X-ray structure of the *trans* DMPE cyclopentadienyl complex confirmed the assignment of a *trans* disposition of the DMPE ligand for one of the isomers, as shown in Fig. 2. The hydride ligands were located and refined isotropically. The small bite angle of 84.7° for the P–Re–P bond angle forces the hydrogen atoms apart (H–Re–H = 146°). These angles can be compared with values of 108.6 and 138°, respectively, for CpRe(PPh_3)$_2H_2$ [4].

Irradiation of a C_6D_6 solution of complex **1** (4.1 mM) in the presence of DPPE (4 equiv.) produces only the *trans*-phosphine isomer, *trans*-CpRe(DPPE)H_2, based upon the splitting of the hydride resonance (t, J=41.3 Hz) in the ^{1}H NMR spectrum (Scheme 1). This result was not surprising in light of the DMPE substitution observation and led to the use of DPPM, the DPPE analog with a methylene bridge in place of the ethylene bridge. The P–P distance in this ligand is not great enough to make the *trans*-phosphine dihydride analog to the DMPE and DPPE complexes. Photolysis of a deuterobenzene solution of **1** (4.1 mM) and DPPM (4 equiv.) through Pyrex produced a single organometallic product with ^{1}H NMR resonances consistent with the assignment *cis*-CpRe(DPPM)H_2 (Table 1, Scheme 1).

To summarize the photochemical behavior of **1** in the presence of chelates, DPPE gives all *trans*-phosphine substitution, DMPE yields a mixture of the *cis* and *trans*-phosphine substitution products in a 1:2 molar ratio, respectively, and DPPM provides the *cis*-phosphine isomer exclusively. Despite the fact that irradiations were carried out in deuterated solvents, there is no loss of the hydride resonance intensity due to partial deuteration of the hydride position.

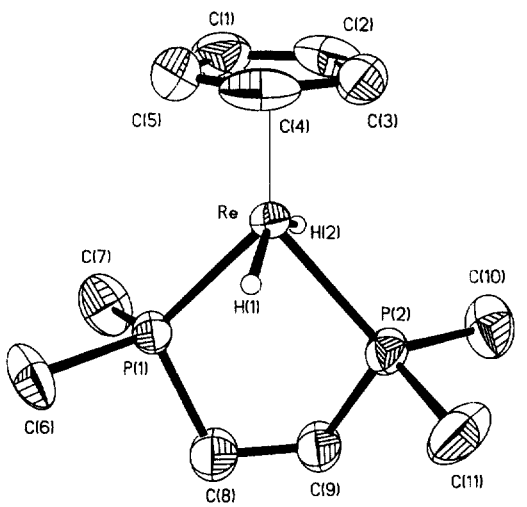

Fig. 2. ORTEP drawing of *trans*-CpRe(DMPE)H_2 with ellipsoids shown at the 50% probability level. Hydrogen atoms attached to carbon have been omitted for clarity. The hydride ligands were located and refined.

Photolysis of a benzene solution of **1** (4.1 mM) and ethylene (20 equiv.) through Pyrex generates the ethylene substituted complex $CpRe(PPh_3)(C_2H_4)H_2$ in yields as high as 40% following 2 h irradiation. Heating this same sample to 80°C for 15 min results in the reverse reaction. Photolysis of a THF-d_8 solution of **1** for 15 min at −70°C in the absence of added ligand showed a doublet in the hydride region at δ −10.11 (J = 11.3 Hz) which disappears upon warming to −20°C. The hydride resonance integrates to 2H relative to 5H for the new resonance observed in the Cp region of the spectrum (δ 4.534). These resonances are assigned as belonging to the unstable THF-d_8 complex, $CpRe(PPh_3)(THF\text{-}d_8)H_2$ (Eq. (3)), which reverts to **1** upon warming. Irradiation of **1** with 2,6-xylylisocyanide (7 equiv.) first produces $CpRe(PPh_3)(CNxylyl)H_2$, but further irradiation produces $CpRe(CNxylyl)_3$ rather than $CpRe(CNxylyl)_2H_2$. An organic product, $H_2C{=}N$-(2,6-xylyl) is also produced.

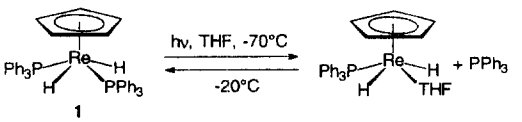

(3)

In summary, irradiation of benzene solutions of $CpRe(PPh_3)_2H_2$ with various two-electron donor ligands provides entry to many new phosphine substituted complexes. The mechanism for phosphine exchange, where L = PMe_3, has been found to be associative, not dissociative [11]. Migration of the hydride to the Cp ring is believed to provide a vacant site for the substitution rather than η^5 to η^3 slippage of the Cp ring, since (η^5-indenyl)$Re(PPh_3)_2H_2$ is totally unreactive with phosphines, either thermally [12] or photochemically [11].

2.3. Photochemical insertion of ethylene into the C–H bond of benzene

As mentioned above, irradiation of a C_6D_6 solution of complex **1** and ethylene results in the formation of up to 40% of the ethylene substituted complex *trans*-$CpRe(PPh_3)(C_2H_4)H_2$ after 2 h. Longer term irradiation (Pyrex filtered UV, 12–48 h) of the solution in the presence of added hydrogen shows ^1H NMR spectroscopic evidence for the catalytic formation of ethylbenzene, ethane, butane and 1-butene (Eq. (4)). In the absence of added H_2, complex **1**

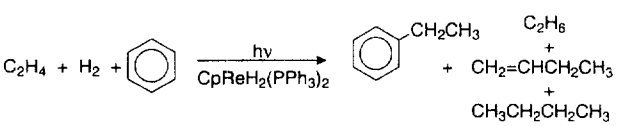

(4)

decomposes as the dihydride ligands are eventually consumed in the production of ethane. Gas chromatographic analysis of the product mixture allowed quantification of these products. Fig. 3 shows turnover numbers after increasing irradiation times of samples containing **1** (6 mM) in benzene under 150 psi ethylene and 1 atm H_2 at room temperature. In an experiment similar to those described by Crabtree et al. to test for the presence of a colloidal catalyst [13], a drop of mercury metal was placed in the tube. Irradiation through Pyrex afforded the same hydrocarbon products observed in the absence of mercury.

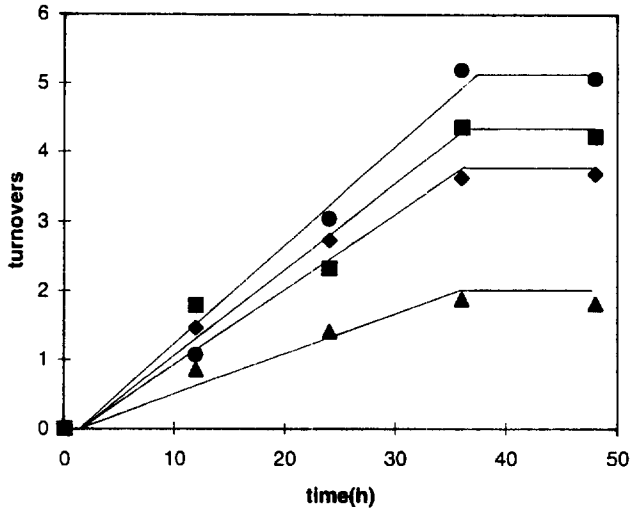

Fig. 3. Products from the photochemical reaction of $CpRe(PPh_3)_2H_2$ with ethylene (150 psi) and H_2 (15 psi) in benzene. (■) Ethylbenzene, (●) ethane, (♦) 1-butene, (▲) butane.

In a related experiment, propylene replaced ethylene. Propane and n-propylbenzene were the only hydrocarbon products identified. After 20 h irradiation only 3 turnovers of propane and 0.8 turnover of propylbenzene were observed.

Several other examples of olefin insertion into aromatic C–H bonds have been reported. Hong and Yamazaki observed coupling of ethylene and benzene to give styrene and H_2 [14]. This reaction is coupled to the reaction of the Rh catalyst with CO and ethylene to give diethylketone. Turnovers of styrene range from 40 to 120 under 30 atm CO and ethylene at 250°C. Also of interest is the report by Sen and Lai of ethylene insertion into the C–H bond of benzene using $[Pd(CH_3CN)_4]^{2+}$. An activated electrophilic ethylene complex is believed to be responsible for the observed attack on benzene. The complex was also a catalyst for ethylene polymerization [15]. Tanaka and co-workers have inserted the activated olefin methyl acrylate into the benzene C–H bond using $RhCl(CO)(PMe_3)_2$. Irradiation of this complex in benzene solution in the presence of olefin gives 24 turnovers of the insertion/β-elimination product methyl cinnamate with a 1.5:1 *trans*:*cis* ratio. 10 turnovers of olefin hydrogenation are also observed [16].

Mares and co-workers have reported the $RhCl_3/PPh_3$ catalyzed insertion of ethylene into the *ortho* C–H bonds of aniline with subsequent oxidation in a complicated sequence to give 2-methylquinoline [17]. The coordination of the aniline nitrogen was believed to direct the insertion of two ethylene molecules into the *ortho* C–H bond. About 10 turnovers of product were observed at 200°C. More recently, Murai et al. have reported the catalytic insertion of substituted olefins into the C–H bonds of aromatic ketones using

$Ru(CO)(PPh_3)_3H_2$. This catalyst demonstrates high *ortho* selectivity (presumably due to coordination of the ketone oxygen) and gives high yields of products with turnover numbers approaching 25 [18].

2.4. Thermal reactions of $CpRe(PPh_3)H_4$ in the presence of phosphines

An alternate preparation for many of the $CpRe(P')_2H_2$ complexes is provided by the thermolysis at 110°C of a benzene solution of $CpRe(PPh_3)H_4$ [4,19], and excess P′ (P′ = *p*-tolyl, PMe_3). ^1H NMR spectroscopic analysis of the reaction progress shows a new hydride doublet resonance for the substitution of PPh_3 by P′ followed by a new triplet due to the slow loss of dihydrogen and coordination of a second P′ to yield complexes of the type $CpRe(P')_2H_2$. The thermolysis of $CpRe(PPh_3)H_4$ at 110°C with PPh_3 results in slow loss of H_2 to produce $CpRe(PPh_3)_2H_2$ as the only product with a half life of about 400 h.

A plot of mole fraction of each organometallic species observed versus time is shown for the reaction of $CpRe(PPh_3)H_4$ with PMe_3 and DMPE in Figs. 4 and 5, respectively. Examination of Fig. 4 indicates that the product obtained by loss of H_2 from $CpRe(PPh_3)H_4$, $CpRe(PPh_3)(PMe_3)H_2$, is a minor product compared to $CpRe(PMe_3)H_4$. The latter is then converted to $CpRe(PMe_3)_2H_2$. With DMPE, the initial phosphine substitution adduct $CpRe(\eta^1\text{-DMPE})H_4$ rapidly undergoes intramolecular displacement of H_2 to close the chelate, so that the mono-phosphine intermediate is not observed.

Scheme 2 summarizes the thermal reactivity of $CpRe(PPh_3)H_4$. Exchange of phosphines is faster than reductive elimination of H_2 during thermolysis at 110°C. In the presence of excess phosphine continued thermolysis results in formation of $CpRe(P')_2H_2$ complexes as the major product observed by ^1H NMR spectroscopy. Using this Scheme, the

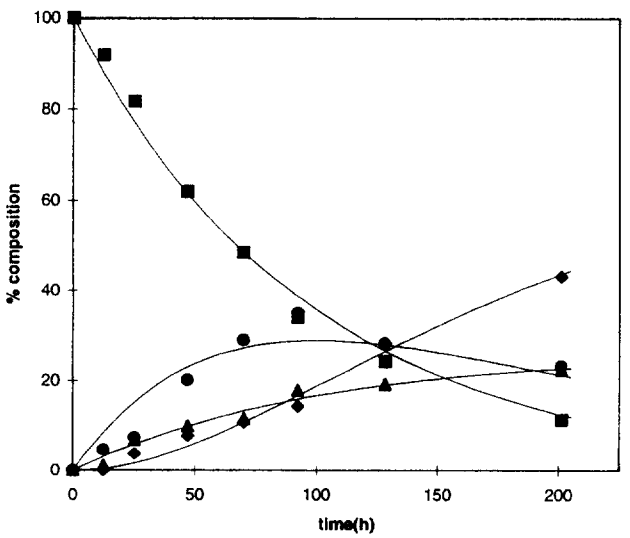

Fig. 4. Thermal reaction of $CpRe(PPh_3)H_4$ with PMe_3 in C_6D_6 at 110°C. (■) $CpRe(PPh_3)H_4$, (●) $CpRe(PMe_3)H_4$, (▲) $CpRe(PPh_3)(PMe_3)H_2$, (◆) $CpRe(PMe_3)_2H_2$.

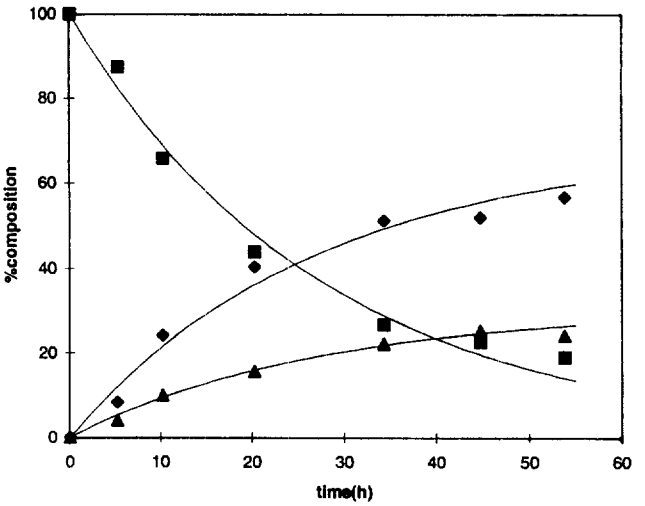

Fig. 5. Thermal reaction of $CpRe(PPh_3)H_4$ with DMPE in C_6D_6 at 110°C. (■) $CpRe(PPh_3)H_4$, (●) *cis*-$CpRe(DMPE)H_2$, (▲) *trans*-$CpRe(DMPE)H_2$.

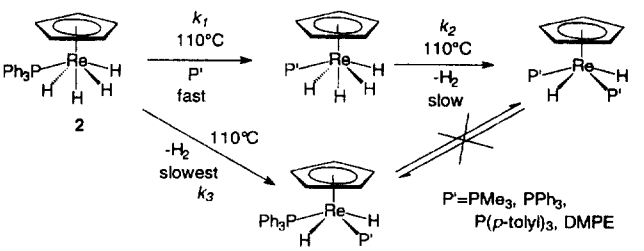

Scheme 2.

exchange data with PMe_3 in Fig. 4 have been fit using a least squares kinetic simulation. The solid lines show the fit using $k_1 = 2.1 \times 10^{-6}\ s^{-1}$, $k_2 = 2.6 \times 10^{-6}\ s^{-1}$ and $k_3 = 7.3 \times 10^{-7}\ s^{-1}$. A similar fit for the DMPE substitution data in Fig. 5 yields $k_1 = 3.0 \times 10^{-6}\ s^{-1}$ and $k_3 = 6.8 \times 10^{-6}\ s^{-1}$. k_2 must be substantially greater than k_1 since the intermediate $CpRe(\eta^1\text{-DMPE})H_4$ is not observed.

2.5. Photolysis of $CpRe(PPh_3)H_4$

When a deuterobenzene solution of $CpRe(PPh_3)H_4$ and PPh_3 or $P(p\text{-tolyl})_3$ (3–5 equiv.) was irradiated through Pyrex, the only organometallic product observed by ^1H NMR spectroscopy was **1** or $CpRe(PPh_3)[P(p\text{-tolyl})_3]H_2$, respectively (Eq. (5)). A singlet at δ 4.459 for dihydrogen is also observed.

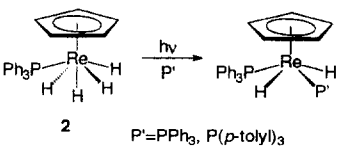

(5)

Irradiation of a C_6D_6 solution containing $CpRe(PPh_3)H_4$ and DMPE (4 equiv.) initially resulted in production of $CpRe(PPh_3)(\eta^1\text{-DMPE})H_2$. Upon continued photolysis of the solution, resonances for free PPh_3, *trans*-$CpRe(DMPE)H_2$ and *cis*-$CpRe(DMPE)H_2$ are observed. Analo-

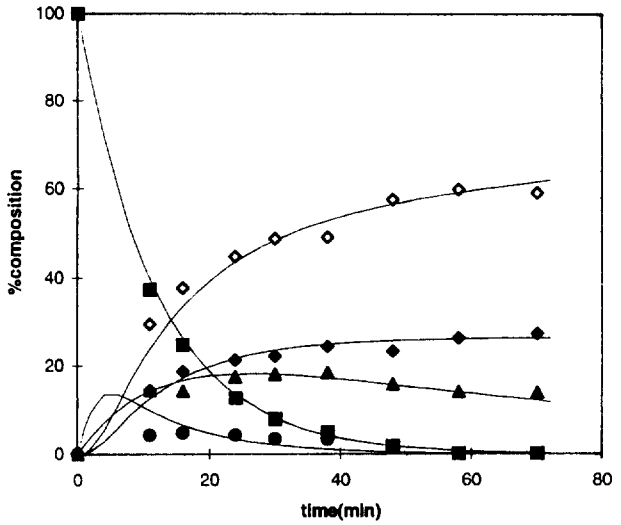

Fig. 6. Photochemical reaction of $CpRe(PPh_3)H_4$ with DMPE in C_6D_6. (■) $CpRe(PPh_3)H_4$, (●) $CpRe(\eta^1\text{-DMPE})H_4$, (▲) $CpRe(\eta^1\text{-DMPE})(PPh_3)H_2$, (◆) *cis*-$CpRe(DMPE)H_2$, (◇) *trans*-$CpRe(DMPE)H_2$.

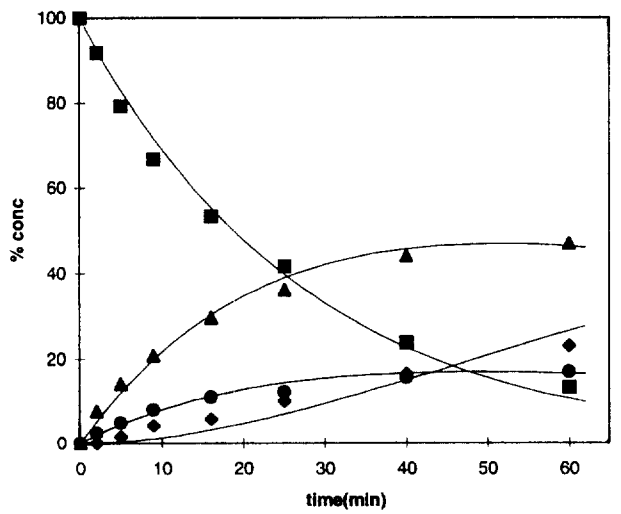

Fig. 7. Photochemical reaction of $CpRe(PPh_3)H_4$ with PMe_3 in C_6D_6. (■) $CpRe(PPh_3)H_4$, (●) $CpRe(PMe_3)H_4$, (▲) $CpRe(PPh_3)(PMe_3)H_2$, (◆) $CpRe(PMe_3)_2H_2$.

gously, irradiation of a C_6D_6 solution containing $CpRe(PPh_3)H_4$ and PMe_3 (10 equiv.) initially resulted in the production of $CpRe(PPh_3)(PMe_3)H_2$. Continued irradiation led to the disubstituted PMe_3 complex, $CpRe(PMe_3)_2H_2$. Only a trace of $CpRe(PMe_3)H_4$ is observed which indicates that phosphine substitution upon irradiation is a minor side reaction compared to H_2 loss. Plots of mole fraction of observed products versus time for irradiation of $CpRe(PPh_3)H_4$ in the presence of DMPE and PMe_3 are shown in Figs. 6 and 7. Each plot clearly shows that $CpRe(PPh_3)(P')H_2$ is an intermediate and that upon continued irradiation the disubstituted phosphine complexes, $CpRe(P')_2H_2$, are the major products.

Scheme 3 summarizes the photochemical reactivity of $CpRe(PPh_3)H_4$. Loss of H_2 is much faster than loss of phosphine during irradiation and in the presence of excess phosphine continued irradiation results in formation of $CpRe(P')_2H_2$ complexes as the only product.

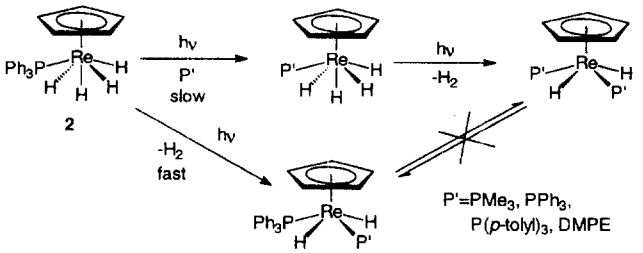

Scheme 3.

3. Experimental

3.1. General considerations

Most compounds used in this work are only slightly air sensitive in the solid state, but are unstable to oxygen and moisture in solution and undergo considerable decomposition over several minutes. All operations were performed under vacuum or in a Vacuum Atmospheres Corp. Dri-lab glove box. Trimethylphosphine, tri-*o*-tolylphosphine, triphenylphosphine and 2,6-xylylisocyanide were purchased from Strem Chemicals. Tetrahydrofuran was distilled from purple solutions of sodium benzophenone ketyl under vacuum. Aliphatic and aromatic hydrocarbon solvents were vacuum distilled from purple solutions of potassium benzophenone ketyl containing a small amount of tetraglyme. Before distillation, aliphatic hydrocarbon solvents were stirred over H_2SO_4 for 48 h, washed successively with sat. $KMnO_4$ in 10% H_2SO_4, three portions of H_2O and one portion of sat. Na_2CO_3, and stored over $CaCl_2$. Benzene-d_6 was obtained from Merck Isotopes division. $CpRe(PPh_3)_2H_2$ and $CpRe(PPh_3)H_4$ were prepared as previously described [5].

High field ^1H NMR spectra were recorded on a Bruker WH-400 NMR spectrometer, and are reported in units of δ (ppm downfield from tetramethylsilane but measured relative to the residual proton resonance in the benzene-d_6 solvent at δ 7.15). Temperature was regulated by a Bruker BVT-1000 temperature control unit, and was calibrated using standard methanol samples.

Photolyses were carried out using a 200 W high pressure mercury arc lamp in an Oriel housing fitted with a focused beam adapter, a water filter to absorb IR, and a 2 inch × 2 inch borosilicate glass filter ($\lambda > 300$ nm). Low temperature photolyses were carried out in a Pyrex dewar. Analytical gas chromatography was performed using a Hewlett-Packard 5710A gas chromatograph with a 6.5 foot × 1/8 inch stainless steel column packed with Poropak Q.

Single crystal X-ray diffraction studies were carried out using an Enraf-Nonius CAD4 diffractometer. Calculations were carried out on a microVAX II GPX workstation using the Molecular Structure Corporation TEXSAN structure analysis software.

3.2. Thermal reaction of 1 with CH_3Br and CH_3I

The complex $CpRe(PPh_3)_2H_2$ (5 mg, 0.006 mmol) was placed under vacuum in an NMR tube. C_6D_6 (0.5 ml) was

vacuum transferred into the tube, followed by CH_3Br (2 equiv.). The tube was sealed and heated to 90°C. A ^1H NMR spectrum recorded after 2 weeks showed only resonances consistent with the new complex $CpRe(Br)(PPh_3)_2H$ and methane. A similar reaction employing CH_3I produced the new complex $CpRe(I)(PPh_3)_2H$.

3.3. Low temperature irradiation of $CpRe(PPh_3)_2H_2$ in THF-d_8

The complex $CpRe(PPh_3)_2H_2$ (3 mg, 0.004 mmol) was placed under vacuum in an NMR tube. THF-d_8 was vacuum distilled into the tube and the tube then sealed. The sample was cooled to −70°C in a methanol/LN_2 bath and irradiated through a Pyrex Dewar. After 15 min irradiation, the sample was transferred to a precooled NMR probe at −70°C and a ^1H NMR spectrum recorded, showing a new doublet resonance in the hydride region at δ −10.110 (J = 11.3 Hz) and a new singlet resonance at 4.534 as well as new resonances for free PPh_3 in the aromatic region. Upon warming the tube to −20°C, a ^1H NMR spectrum showed the disappearance of these resonances and the presence of only the starting material (Table 1).

3.4. Irradiation of $CpRe(PPh_3)_2H_2$ with PMe_3

The complex $CpRe(PPh_3)_2H_2$ (1.5 mg, 0.0018 mmol) was placed under vacuum in an NMR tube. C_6D_6 (0.4 ml) was vacuum transferred into the tube followed by PMe_3 (20 equiv.) and the tube sealed. The sample was irradiated through a 328 nm bandpass filter. A ^1H NMR spectrum recorded after irradiation showed new resonances consistent with free PPh_3 and the monosubstituted complex $CpRe(PPh_3)(PMe_3)H_2$. Further irradiation resulted in the appearance of resonances for the disubstituted complex $CpRe(PMe_3)_2H_2$ (Table 1).

3.5. Irradiation of $CpRe(PPh_3)_2H_2$ with P(p-tolyl)$_3$ and PMe_2Ph

The complex $CpRe(PPh_3)_2H_2$ (1.5 mg, 0.0018 mmol) and P(*p*-tolyl)$_3$ (3 mg, 10 mmol) were placed under vacuum in an NMR tube. C_6D_6 (0.4 ml) was vacuum distilled into the tube and the tube sealed. The sample was irradiated through a 328 nm bandpass filter. ^1H NMR spectra were recorded periodically, showing resonances for the monosubstitution product $CpRe(PPh_3)[P(p\text{-tolyl})_3]H_2$ followed by the disubstitution product $CpRe[P(p\text{-tolyl})_3]_2H_2$. Similar observations were made with PMe_2Ph (Table 1).

3.6. Independent preparation of $CpRe(PMe_2Ph)_2H_2$

To a solution of 50 mg of $Re(PMe_2Ph)_3H_5$ in 5 ml of benzene was added 0.1 ml of freshly cracked cyclopentadiene. Photolysis of the sample through a 345 LP filter gave a mixture of $CpRe(PMe_2Ph)_2H_2$ and $CpRe(PMe_2Ph)H_4$ (8:1). Recrystallization from hexane at −20°C separated $CpRe(PMe_2Ph)_2H_2$ as pale yellow needles.

3.7. Irradiation of $CpRe(PPh_3)_2H_2$ with DMPE

The complex $CpRe(PPh_3)_2H_2$ (1.5 mg, 0.018 mmol) was placed under vacuum in an NMR tube. C_6D_6 (0.4 ml) was vacuum distilled into the tube followed by DMPE (4 equiv.) and the tube was sealed. The sample was irradiated through a 328 nm bandpass filter, and ^1H NMR spectra were recorded periodically. New resonances were seen first for the η^1-DMPE complex *trans*-$CpRe(PPh_3)(\eta^1\text{-DMPE})H_2$ and then for the disubstituted complexes *trans*-$CpRe(DMPE)H_2$ and *cis*-$CpRe(DMPE)H_2$ (Table 1).

3.8. Irradiation of $CpRe(PPh_3)_2H_2$ with DPPE

The complex $CpRe(PPh_3)_2H_2$ (1.5 mg, 0.0018 mmol) and DPPE (3 mg, 0.0075 mmol) were placed under vacuum in an NMR tube. C_6D_6 (0.4 ml) was vacuum distilled into the tube and the tube sealed. The sample was irradiated through a 328 nm bandpass filter, and ^1H NMR spectra were recorded periodically. New resonances were seen for free PPh_3 and for the monosubstitution product *trans*-$CpRe(PPh_3)(\eta^1\text{-DPPE})H_2$, followed by the appearance of resonances for the disubstituted product *trans*-$CpRe(DPPE)H_2$ (Table 1).

3.9. Irradiation of $CpRe(PPh_3)_2H_2$ with CO

The complex $CpRe(PPh_3)_2H_2$ (1.5 mg, 0.0018 mmol) was placed under vacuum in an NMR tube. C_6D_6 (0.4 ml) was vacuum distilled into the tube and the tube then sealed under 700 torr CO. The sample was irradiated through a 328 nm bandpass filter, and ^1H NMR spectra were recorded periodically. New resonances were seen for PPh_3 and the monosubstitution product *trans*-$CpRe(PPh_3)(CO)H_2$, followed by the formation of the disubstituted product *trans*-$CpRe(CO)_2H_2$ (Table 1).

3.10. Irradiation of $CpRe(PPh_3)_2H_2$ with 2,6-xylylisocyanide

The complex $CpRe(PPh_3)_2H_2$ (1.5 mg, 0.0018 mmol) and 2,6-xylylisocyanide (2 mg, 0.017 mmol) were placed under vacuum in an NMR tube. C_6D_6 (0.4 ml) was vacuum distilled into the tube and the tube sealed. The sample was irradiated through a 328 nm bandpass filter, and ^1H NMR spectra were recorded periodically. New resonances were seen for PPh_3 and the monosubstitution product *trans*-$CpRe(PPh_3)(CN\text{-}2,6\text{-xylyl})H_2$, followed by resonances for $CpRe(CN\text{-}2,6\text{-xylyl})_3$ and H_2CN-2,6-xylyl upon continued irradiation (Table 1).

3.11. Irradiation of $CpRe(PPh_3)_2H_2$ with C_2H_4

The complex $CpRe(PPh_3)_2H_2$ (1.5 mg, 0.018 mmol) was placed under vacuum in an NMR tube. C_6D_6 (0.4 ml) was

vacuum transferred into the tube followed by C_2H_4 (20 equiv.) and the tube sealed. The sample was irradiated through a 328 nm bandpass filter, and ^1H NMR spectra were recorded periodically. New resonances were seen for free PPh_3 and for the monosubstituted complex $CpRe(PPh_3)(C_2H_4)H_2$, in 40% yield. The sample was then heated to 80°C for 15 min. ^1H NMR spectroscopic analysis of the sample showed the formation of **1** and free C_2H_4. No free PPh_3 was observed.

3.12. Irradiation of $CpRe(PPh_3)_2H_2$ with C_2H_4 and H_2 in C_6H_6

For these reactions, a quartz high pressure Fischer-Porter type reaction vessel was used for all irradiations. The bomb was charged with $CpRe(PPh_3)_2H_2$ (3 mg, 0.004 mmol) and a stirbar along with 1 ml C_6H_6. The solution was freeze-pump-thaw degassed and ethylene introduced (150 psi, 25°C). The solution was then cooled in liquid nitrogen (to condense the ethylene gas) and 1 atm H_2 introduced. The solution was thawed, resulting in a total pressure of 165–170 psi. The sample was irradiated through a 328 nm bandpass filter while maintaining the temperature at 25°C. GC analysis of the sample was made by expansion of all of the volatile products and solvent into a 6.8 l evacuated chamber, using added propane as an internal standard, and withdrawing 100 ml aliquots of gas for analysis. The bomb reactor was freshly charged for each of the irradiation times shown in Fig. 3, producing the product amounts shown.

3.13. Thermal reaction of $CpRe(PPh_3)H_4$ with PMe_3, $P(p\text{-tolyl})_3$, DMPE, DPPM, DPPE and PPh_3

The complex $CpRe(PPh_3)H_4$ (1 mg, 0.002 mmol) and the phosphine (4–20 equiv.) were placed in an NMR tube. C_6D_6 (0.4 ml) was vacuum distilled into the tube and the tube sealed. The sample was heated to 90°C and the reaction progress monitored by ^1H NMR spectroscopy. Integration of the hydride resonances for each of the product complexes was used to determine the molar ratio of each product at varying reaction times. Data for the distribution of species in the reactions with PMe_3 and DMPE are given in Figs. 4 and 5.

3.14. Photochemical reaction of $CpRe(PPh_3)H_4$ with PMe_3, $P(p\text{-tolyl})_3$, DMPE and PPh_3

The complex $CpRe(PPh_3)H_4$ (1 mg, 0.002 mmol) and the phosphine (3–10 equiv.) were placed in an NMR tube. C_6D_6 (0.4 ml) was vacuum distilled into the tube and the tube sealed. The sample was irradiated through a 328 nm bandpass filter and the reaction progress monitored by ^1H NMR spectroscopy. The ^1H NMR spectra were consistent with the loss of H_2 from $CpRe(PPh_3)H_4$ and substitution of the hydride ligands with one phosphine, followed by substitution of the PPh_3 ligand by a second phosphine (or chelate in the case of DMPE). Integration of the hydride resonances for each of the product complexes was used to determine the molar ratio of each product at varying reaction times. Data

Table 2
Crystal and data collection parameters for *trans*-$CpRe(PMe_2Ph)_2H_2$ and *trans*-$CpRe(DMPE)H_2$

Compound	*trans*-$CpRe(PMe_2Ph)_2H_2$	*trans*-$CpRe(DMPE)H_2$
Chemical formula	$ReP_2C_{21}H_{29}$	$ReP_2C_{11}H_{23}$
Formula weight	529.61	403.46
Crystal system	monoclinic	monoclinic
Space group (No.)	$P2_1/n$ (No. 14)	$P2_1/n$ (No. 14)
Z	4	4
a (Å)	7.467(3)	6.249(6)
b (Å)	23.874(14)	16.671(8)
c (Å)	11.798(6)	13.867(7)
β (°)	100.16(4)	92.11(6)
V (Å^3)	2070.2(3.5)	1443.7(2.9)
Temperature (°C)	−75	−41.5
ρ_{calc} (g cm^{-3})	1.70	1.86
Crystal dimensions (mm)	0.10×0.15×0.35	0.15×0.25×0.36
Diffractometer (geometry)	Enraf Nonius CAD4 (2θ–ω)	Enraf Nonius CAD4 (2θ–ω)
Radiation (Å), monochromater	Mo Kα (0.71073), graphite	Mo Kα (0.71073), graphite
2θ Range (°)	4–50	4–50
Data collected	$+h, +k, \pm l$	$+h, +k, \pm l$
No. data collected	4033	2170
No. unique data ($F^2 > 3\sigma(F^2)$)	2982	1486
No. parameters varied	225	135
Absorption correction	semi-empirical (DIFABS)	semi-empirical (DIFABS)
Range transmission factors	0.75–1.48	0.70–1.32
μ (cm^{-1})	63.64	87.19
$R(F_o)$	0.0293	0.0248
$R_w(F_o)$	0.0387	0.0290
Goodness-of-fit	1.23	1.29

Table 3
Selected distances (Å) and angles (°) for *trans*-CpRe(PMe_2Ph)$_2H_2$ and *trans*-CpRe(DMPE)H_2

	CpRe(PMe_2Ph)$_2H_2$	CpRe(DMPE)H_2
Re–P(1)	2.302(2)	2.296(2)
Re–P(2)	2.289(2)	2.282(3)
Re–H(1)	1.59(5)	1.44(7)
Re–H(2)	1.69(6)	1.5(1)
P(1)–Re–P(2)	103.00(7)	84.75(8)
P(1)–Re–H(1)	64(2)	81(3)
P(1)–Re–H(2)	71(2)	78(4)
P(2)–Re–H(1)	77(2)	81(3)
P(2)–Re–H(2)	76(2)	70(4)
H(1)–Re–H(2)	120(3)	146(5)

for the distribution of species in the reactions with PMe_3 and DMPE are given in Figs. 6 and 7.

3.15. X-ray structural determination of trans-CpRe(PMe_2Ph)$_2H_2$

A single colorless crystal of the complex was mounted with epoxy on a glass fiber, cooled to −75°C in a stream of nitrogen, and cell constants obtained from 25 centered reflections with values of χ between 0 and 70°. Routine data collection of one quadrant of data was undertaken on the primitive monoclinic cell as indicated in Table 2. The Molecular Structure Corporation TEXSAN analysis software package was used for data reduction and solution [1]. Patterson map solution of the structure to locate the rhenium atom, followed by expansion of the structure with the program DIRDIF revealed all non-hydrogen atoms. Following isotropic refinement, an absorption correction was applied using the program DIFABS. Full-matrix least-squares anisotropic refinement of all non-hydrogen atoms (with hydrogens attached in idealized positions) was carried out to convergence. At this point, a difference Fourier map showed the two highest peaks in reasonable positions for the hydride ligands. Both the positions and isotropic thermal parameters for the hydride ligands were refined in the final model. Selected distances and angles are given in Table 3 and fractional coordinates in Table 4.

3.16. X-ray structural determination of trans-CpRe(DMPE)H_2

A single colorless crystal of the complex was mounted with epoxy on a glass fiber, cooled to −41.5°C in a stream of nitrogen, and cell constants obtained from 25 centered reflections with values of χ between 0 and 70°. Routine data collection of one quadrant of data was undertaken on the primitive monoclinic cell as indicated in Table 2. The structure was solved and refined as described for CpRe(PMe_2Ph)$_2H_2$ above. Both the positions and isotropic thermal parameters for the hydride ligands were refined in the final model. Selected distances and angles are given in Table 3 and fractional coordinates in Table 5.

[1] $R_1 = \{\Sigma||F_o| - |F_c||\}/\{\Sigma|F_o|\}$; $R_2 = [\Sigma w(|F_o| - |F_c|)^2]^{1/2}/\{\Sigma wF_o^2\}$, where $w = [\sigma^2(F_o) + (\rho F_o^2)^2]^{1/2}$ for the non-Poisson contribution weighting scheme. The quantity minimized was $\Sigma w(|F_o| - |F_c|)^2$. Source of scattering factors f_o, f', f'' [20].

Table 4
Positional parameters and B_{eq} of refined atoms for *trans*-CpRe(PMe_2Ph)$_2H_2$

Atom	x	y	z	B_{eq} (Å^2)
Re	0.22045(3)	0.138468(9)	0.22045(2)	1.98(1)
P1	0.1269(2)	0.20269(6)	0.3433(1)	2.33(5)
P2	0.1463(2)	0.05453(6)	0.2937(1)	2.13(5)
C1	0.1994(9)	0.1597(3)	0.0290(5)	3.2(3)
C2	0.277(1)	0.1075(3)	0.0515(5)	3.5(3)
C3	0.443(1)	0.1148(4)	0.1273(7)	5.2(4)
C4	0.458(1)	0.1742(5)	0.1517(6)	6.4(5)
C5	0.308(1)	0.2001(3)	0.0892(6)	4.3(3)
C6	0.304(1)	0.2498(3)	0.4160(5)	3.7(3)
C7	−0.041(1)	0.2541(3)	0.2784(5)	3.7(3)
C8	0.0188(7)	0.1784(2)	0.4629(4)	2.2(2)
C9	−0.1613(8)	0.1613(3)	0.4414(5)	3.0(2)
C10	−0.247(1)	0.1406(3)	0.5286(6)	3.3(3)
C11	−0.150(1)	0.1372(3)	0.6400(6)	3.7(3)
C12	0.031(1)	0.1536(3)	0.6623(5)	3.4(3)
C13	0.1147(8)	0.1742(3)	0.5742(4)	2.7(2)
C14	0.215(1)	0.0388(3)	0.4467(5)	3.8(3)
C15	−0.0929(9)	0.0322(3)	0.2754(6)	3.6(3)
C16	0.2477(7)	−0.0045(3)	0.2290(4)	2.2(2)
C17	0.1558(8)	−0.0320(3)	0.1321(4)	2.9(2)
C18	0.235(1)	−0.0746(3)	0.0804(5)	3.9(3)
C19	0.406(1)	−0.0922(3)	0.1259(6)	4.1(3)
C20	0.503(1)	−0.0648(3)	0.2219(7)	4.6(3)
C21	0.4244(8)	−0.0222(3)	0.2723(5)	3.4(3)
H1	0.336(7)	0.137(2)	0.348(4)	0(1)
H2	−0.010(8)	0.139(2)	0.198(5)	2(1)

Table 5
Positional parameters and B_{eq} of refined atoms for *trans*-CpRe(DMPE)H_2

Atom	x	y	z	B_{eq} (Å^2)
Re	0.11071(5)	0.10815(2)	0.79449(2)	3.23(2)
P1	0.2219(4)	0.1354(1)	0.6420(1)	4.1(1)
P2	0.2052(4)	−0.0208(1)	0.7608(2)	4.8(1)
C1	0.144(2)	0.2147(7)	0.8900(8)	7.0(7)
C2	0.155(2)	0.148(1)	0.9469(7)	7.1(7)
C3	−0.044(3)	0.1085(6)	0.9393(8)	7.8(7)
C4	−0.169(2)	0.1561(9)	0.8772(8)	6.6(6)
C5	−0.053(2)	0.2194(7)	0.8479(7)	6.3(6)
C6	0.048(2)	0.1816(8)	0.5518(6)	7.1(6)
C7	0.462(2)	0.1925(8)	0.6251(8)	8.2(7)
C8	0.278(2)	0.0402(7)	0.5817(7)	7.9(7)
C9	0.347(2)	−0.0224(6)	0.6460(7)	7.4(6)
C10	0.399(2)	−0.0738(7)	0.8372(8)	7.7(6)
C11	−0.002(2)	−0.0967(6)	0.743(1)	8.5(7)
H1	−0.08(1)	0.084(4)	0.741(5)	4(2)
H2	0.36(2)	0.098(6)	0.806(7)	10(3)

4. Supplementary material

Supplementary material available includes a complete listing of tables of distances and angles, fractional atomic coor-

dinates, and thermal parameters for $CpRe(PMe_2Ph)_2H_2$ and $CpRe(DMPE)H_2$ (10 pages).

Acknowledgements

Acknowledgment is made to the US Department of Energy Office of Basic Energy Sciences (FG02-86ER13569) for their support of this work.

References

[1] D. Baudry, M. Ephritikhine and H. Felkin, J. Chem. Soc., Chem. Commun., (1980) 1243.
[2] D. Baudry, M. Ephritikhine and H. Felkin, J. Chem. Soc., Chem. Commun., (1980) 249.
[3] W.D. Jones and J.A. Maguire, Organometallics, 5 (1986) 590–591.
[4] W.D. Jones and J.A. Maguire, Organometallics, 6 (1987) 1728–1737.
[5] W.D. Jones and J.A. Maguire, Organometallics, 6 (1987) 1301–1311.
[6] M.R. Detty and W.D. Jones, J. Am. Chem. Soc., 109 (1987) 5666–5673.
[7] R.G. Bergman, P.F. Seidler and T.T. Wenzel, J. Am. Chem. Soc., 107 (1985) 4358.
[8] P.R. Brown, F.G.N. Cloke, M.L.H. Green and N.J. Hazel, J. Chem. Soc., Dalton Trans., (1983) 1075–1079.
[9] M. Canestrari, M.L.H. Green and A. Izquierdo, J. Chem. Soc., Dalton Trans., (1984) 2795–2801.
[10] I. de los Ríos, T. Jiménez, J. Padilla, M.C. Puerta and P. Valerga, Organometallics, 15 (1996) 4565–4574.
[11] J.A. Maguire, Ph.D. Thesis, University of Rochester, 1986; W.D. Jones, J.A. Maguire and G.P. Rosini, Organometallics, to be submitted.
[12] G.P. Rosini and W.D. Jones, J. Am. Chem. Soc., 115 (1993) 965–974.
[13] R.H. Crabtree, J.M. Mihelcic, M.F. Mellea and J.M. Quirk, J. Am. Chem. Soc., 104 (1982) 107–113.
[14] P. Hong and H. Yamazaki, J. Mol. Cat., 76 (1984) 297–311.
[15] A. Sen and T.-W. Lai, J. Am. Chem. Soc., 103 (1981) 4627–4629.
[16] K. Sasaki, T. Sakakura, Y. Tokunaga, K. Wada and M. Tanaka, Chem. Lett., (1988) 685–688.
[17] S.E. Diamond, A. Szalkiewicz and F. Mares, J. Am. Chem. Soc., 101 (1979) 490–491.
[18] S. Murai, F. Kakiuchi, S. Sekine, Y. Tanaka, A. Kamatani, M. Sonoda and N. Chatani, Nature, 366 (1993) 592–531; Bull. Chem. Soc. Jpn., 68 (1995) 62–83.
[19] M.A. Green, J.C. Huffman, K.G. Caulton, W.K. Rybak and J.J. Ziolkowski, J. Organomet. Chem., 218 (1981) C39–C43.
[20] D.T. Cromer and J.T. Waber, International Tables for X-Ray Crystallography, Vol. IV, Kynoch Press, Birmingham, UK, 1974, Tables 2.2B and 2.3.1.